Prediction of the Heat Release Rate of Wood

WILLIAM J. PARKER
Center for Fire Research
National Bureau of Standards, USA

ABSTRACT

A method for predicting the heat release rate of wood for different thicknesses, moisture contents, and exposure conditions is described. A model has been set up and calculations have been made on a microcomputer. Heat release rates and effective heats of combustion were measured as a function of time and external radiant flux on 12.5 mm thick dry vertical specimens of Douglas fir particle board. The calculated and measured curves are similar in shape and amplitude but differ significantly in time scale. The initial results with the model are promising.

INTRODUCTION

The model described in this paper embodies most of the features of the mass loss rate model originally developed by Kung [1] and modified by Taminini [2] and Atreya [3]. The chief distinguishing features of the present model over that of Atreya are: (1) it takes char shrinkage parallel and normal to the surface into account, (2) the thermal properties are a function of temperature and degree of char, (3) it allows for several components of the wood each with different decomposition rate constants, and (4) it takes the change in the heat of combustion of the volatiles for each of the components as a function of its individual degree of char into account.

This paper will describe the model and show some calculations and comparisons with the heat release rate and effective heat of combustion measured in the cone calorimeter [4]. For a more detailed discussion of the model and the experimental procedures see reference [5].

HEAT RELEASE RATE MODEL

The heat release rate model (1) breaks the specimen down into thin slices parallel to the surface as seen in figure 1, (2) calculates the mass loss rate for each slice, (3) multiplies this rate by the local heat of combustion of the volatiles generated, and (4) sums these contributions over the depth of the specimen to obtain the total heat release rate assuming complete combustion of the volatiles leaving the front surface.

The boundaries of each slice move as the specimen shrinks during the burning period so that no solid material crosses a boundary. The rear surface is impervious to mass flow. Flow into the cooler region of the specimen followed by condensation and subsequent evaporation is not treated here. All of the

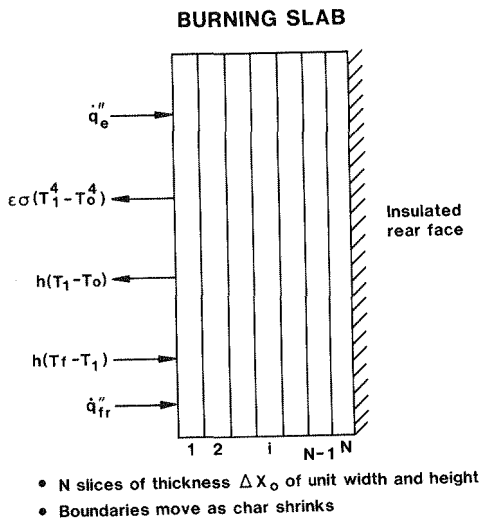

FIGURE 1. Boundary conditions and subdivision of the burning vertical slab.

volatiles pass through the front surface. The transit time of the volatiles from their generation site to the surface is neglected. However, the internal convective heat transfer coefficient is assumed to be so large that the volatiles are maintained in thermal equilibrium with the char through which they pass. Secondary chemical reactions with the char layer are neglected.

The rate of mass generation is expressed as a function of the temperature and the mass retention fraction for each component in each slice using an Arrhenius type expression. The temperature profile as a function of time is calculated from the energy equation using the finite difference method. The rate of change of enthalpy, heat conduction, internal heat generation or absorption and convective cooling by the flow of volatiles are taken into account. However, the convective cooling by the volatiles is cut off in the fully developed char layer since it is assumed that the gases will flow internally to the fissures and exit the specimen from there. The thermal properties are assumed to be a function of the temperature and the total mass retention fraction of each slice. The instantaneous mass retention fraction profile is determined by accounting for the cumulative loss of volatiles.

An adiabatic boundary condition is assumed at the rear surface while the front face is exposed to a constant external radiant flux. Both of these conditions can be made more general later if desired. The front surface also loses heat by reradiation. Up to the time of ignition it also loses heat by laminar free convection. After ignition the convective heat transfer from the flame to the surface is taken into account along with flame radiation. The convective heat transfer coefficient both before and after ignition is multiplied by the blowing factor due to the flow of volatiles through the surface.

Ignition is assumed to occur when the calculated total heat release rate reaches 30 kW/m^2 which is near the minimum heat release rate required to maintain a

flame on the surface. The flame is extinguished when the calculated heat release rate again drops below 30 kW/m^2 at the end of the flaming phase. Only the heat release rate during the flaming phase is treated by this model. During this period oxygen is assumed to be excluded from the solid. The oxidation of the surface prior to ignition and after flaming ceases is not considered.

The mass retention fraction Z_i for each slice is defined by

$$Z_i = m_i/m_i^o = \frac{\rho}{\rho_o} \ell_x \ell_y \ell_z \qquad (1)$$

where m_i is the mass of each slice on an oven dry basis, ρ is its density, and ℓ_x, ℓ_y, and ℓ_z are the contraction factors (i.e., the ratios of the thickness, width and height of the slice to their original values). The superscript and subscript o refer to the initial values.

The contributions of the individual wood components (cellulose, hemicellulose and lignin) are additive so that

$$Z_i = \sum_{k=1}^{n} Z_{i,k} \qquad (2)$$

where $Z_{i,k}$ is the mass of the k th component of the i th slice divided by the original mass of the whole slice. It is necessary to know the reaction rate and heat of combustion of the volatiles for each component as a function of the temperature, T_i, and the component mass retention fraction, $Z_{i,k}/Z_k^o$. Here Z_k^o is the original mass fraction of the k th component.

The moisture is taken into account by assigning a moisture retention fraction,

$$Z_{w_i} = m_{w_i}/m_i^o \qquad (3)$$

where m_{w_i} is the mass of adsorbed water located in slice i at any time.

The mass loss rate and heat release rate per unit area of the original specimen are calculated by the following formulas:

$$\dot{m}'' = \rho_o \frac{\Delta x_o}{\Delta t} \sum_{i=1}^{N} \left(Z_i^t - Z_i^{t+\Delta t}\right) \qquad (4)$$

and

$$\dot{q}''_{rel} = \rho_o \frac{\Delta x_o}{\Delta t} \sum_{i=1}^{N} F_i^t \left(Z_i^t - Z_i^{t+\Delta t}\right) \qquad (5)$$

where the heat of combustion of the volatiles is given by

$$F_i^t = \sum_{k=1}^{n} F_{i,k}^t \, Z_{i,k}^t / Z_i^t \, . \qquad (6)$$

The energy equation is first solved for the temperature. Then the rate equations are used to update the mass retention fraction for each component. The total mass retention fraction, Z_i, for each slice is substituted back into

the energy equation which is then solved for the temperature at the next time step.

The increase in enthalpy of an interior slice is equal to the heat conducted in minus the heat conducted out minus the heat absorbed by the pyrolysis gases passing through on their way to the front surface minus or plus the heat absorbed or generated by pyrolysis and evaporation. The energy equation for an interior slice can be written,

$$\rho_o \Delta x_o \left[\left(Z_i^{t+\Delta t} C_i + Z_{w_i}^{t+\Delta t} C_{w_i}\right) T_i^{t+\Delta t} - \left(Z^t{}_i C_i + Z^t{}_{w_i} C_{w_i}\right) T_i^t\right]$$

$$= K_i \left(\frac{T_{i-1}^{t+\Delta t} - T_i^{t+\Delta t}}{\Delta X} - \frac{T_i^{t+\Delta t} - T_{i+1}^{t+\Delta t}}{\Delta X}\right) \Delta t \, \ell_y \ell_z$$

$$+ \left(C_{g_i} \dot{m}''_{i+1} + C_{w_i} \dot{m}''_{w_{i+1}}\right) \left(\frac{T_{i+1}^{t+\Delta t} + T_i^{t+\Delta t}}{2}\right) \Delta t$$

$$-\left(C_{g_i} \dot{m}''_i + C_{w_i} \dot{m}''_{w_i}\right) \left(\frac{T_i^{t+\Delta t} + T_{i-1}^{t+\Delta t}}{2}\right) \Delta t$$

$$- h_{p_i} \rho_o \Delta x_o \left(Z_i^t - Z_i^{t+\Delta t}\right) - L_v \rho_o \Delta x_o \left(Z_{w_i}^t - Z_{w_i}^{t+\Delta t}\right) \tag{7}$$

where $$\dot{m}''_i = \frac{\rho_o \Delta x_o}{\Delta t} \sum_{j=i}^{N} \left(Z_j^t - Z_j^{t+\Delta t}\right), \tag{8}$$

$$\dot{m}''_{w_i} = \frac{\rho_o \Delta x_o}{\Delta t} \sum_{j=i}^{N} \left(Z_{w_j}^t - Z_{w_j}^{t+\Delta t}\right) \tag{9}$$

and $$h_{p_i} = \sum_{k=1}^{n} \frac{Z_{i,k}^t}{Z_i^t} h_{p_k} . \tag{10}$$

Here $\dot{m}''$ refers to the mass flow per unit original area of the specimen not the contracted area. The heat of pyrolysis of the slice, h_{p_i}, is equal to the weighted averages of the heat of pyrolysis of each component.

Radiative and convective heat transfer must be taken into account at the front surface (i=1). Radiation exchange with the external environment is assumed to take place at the surface. The exchange of radiation between interior slices is considered to be one component of the thermal conductivity. Prior to ignition the surface is cooled by laminar free convection. After ignition it is heated by the flame. The front surface temperature, T_s, for these calculations is obtained by linear extrapolation from the center points of the two slices nearest the surface

$$T_s = \frac{3}{2} T_1 - \frac{1}{2} T_2 . \tag{11}$$

The reradiation from the front surface is given by

$$\alpha\sigma\left(T_s^4 - T_o^4\right) = \alpha\sigma\left(T_s^2 + T_o^2\right)\left(T_s + T_o\right)\left(T_s - T_o\right). \tag{12}$$

The energy flow across the front surface is given by

$$\dot{q}''_{net} = \dot{q}''_e + \dot{q}''_{fR} - \omega\left(T_s - T_o\right) + h_f\left(T_f - T_s\right) B/(\exp(B) - 1) \tag{13}$$

where

$$\omega = \alpha\sigma\left(T_s^2 + T_o^2\right)\left(T_s + T_o\right) + h\, B/(\exp(B)-1)\ . \tag{14}$$

The other quantities are identified as follows: h is the convective heat transfer coefficient from the surface to the ambient air which drops to zero after ignition, h_f is the convective heat transfer coefficient from the flame to the surface which is equal to zero prior to ignition, T_f is the flame temperature, and

$$B = \dot{m}''C_g/h \tag{15}$$

and thus accounts for blowing. Prior to ignition the radiant heat flux from the flame, $\dot{q}''_{fr}$, is zero. The energy equation for the first slice is given by

$$\rho_o \Delta x_o \left[\left(Z_1^{t+\Delta t} C_1 + Z_{w_1}^{t+\Delta t} C_{w_1}\right) T_1^{t+\Delta t} - \left(Z_1^t C_1 + Z_{w_1}^t C_{w_1}\right) T_1^t\right] =$$

$$\left[\dot{q}''_e + \dot{q}''_{fR} - \omega\left(\frac{3}{2} T_1^{t+\Delta t} - \frac{1}{2} T_2^{t+\Delta t} - T_o\right) + h_f\left(T_f - \frac{3}{2} T_1^{t+\Delta t} + \frac{1}{2} T_2^{t+\Delta t}\right) B/(\exp(B)-1)\right.$$

$$\left. - K_1 \ell_z \ell_y \frac{T_1^{t+\Delta t} - T_2^{t+\Delta t}}{\Delta x}\right]\Delta t$$

$$+ \left(C_{g_1} \dot{m}''_2 + C_{w_1} \dot{m}''_{w_2}\right)\left[\frac{T_2^{t+\Delta t} + T_1^{t+\Delta t}}{2}\right]\Delta t$$

$$- \left(C_{g_1} \dot{m}''_1 + C_{w_1} \dot{m}''_{w_1}\right)\left[\frac{3}{2} T_1^{t+\Delta t} - \frac{1}{2} T_2^{t+\Delta t}\right]\Delta t$$

$$- h_{p_1} \rho_o \Delta x_o \left(Z_1^t - Z^{t+\Delta t}\right) - L_v \rho_o \Delta x_o \left(Z_{w_1}^t - Z_{w_1}^{t+\Delta t}\right) \tag{16}$$

The change in mass retention fraction for each component of slice i during the time step is given by

$$Z_{i,k}^{t+\Delta t} - Z_{i,k}^t = -\left(Z_{i,k}^t - Z_{f,k}\right) A_k \exp\left(-E_k/RT_i^{t+\Delta t}\right) \Delta t \tag{17}$$

where $Z_{f,k}$ is the residual mass fraction of component k when pyrolysis is completed in an inert atmosphere and A_k and E_k are the frequency factor and activation energy for component k. The total mass retention fraction for slice i is then given by

$$Z_i^{t+\Delta t} = Z_i^t + \sum_{k=1}^{n} (Z_{i,k}^{t+\Delta t} - Z_{i,k}^t). \quad (18)$$

The change in the mass retention fraction for water during the time step is given by

$$Z_{w_i}^{t+\Delta t} - Z_{w_i}^t = - Z_{w_i}^t A_w \exp\left(- E_w / RT_i^{t+\Delta t}\right)\Delta t \quad (19)$$

These numerical equations were solved on a microcomputer. The parameters - K, ρ, C, C_w, C_g, α, A_k, A_w, E_k, E_w, F_k, h_{pk}, L_v, ℓ_x, ℓ_y, and ℓ_z - are needed as input to the computer model. While some of these data can be obtained within the accuracy needed by consulting the literature the thermophysical properties (K, ρ, α, ℓ_x, ℓ_y and ℓ_z) and the thermochemical properties (A_k, E_k, and F_k) were determined experimentally for the material of concern. Most of these parameters vary with temperature and mass retention fraction. For a discussion of the experimental methods see reference 5.

VERIFICATION WITH THE HEAT RELEASE RATE CALORIMETER

The input parameters along with their assigned values and sources for Douglas fir particle board are listed in Table 1. The front and rear surface temperatures, the mass loss rate, the heat release rate and the effective heat of combustion are all calculated as a function of time. The calculated and experimental curves for the heat release rate and the effective heat of combustion of a dry 12.7 mm specimen of Douglas fir particle board exposed at an external radiant flux of 50 kW/m^2 are compared in figures 2 and 3. The experimental curves were obtained with the cone calorimeter in the vertical orientation.

The calculated heat release rate curve jumps from zero to 30 kW/m^2 at ignition and continues to rise quickly to a sharp peak followed by a rapid decline to a minimum. A second large peak occurs when the thermal wave is reflected from the insulated rear face causing a more rapid rise in the average temperature of the slab. The second peak would be missing altogether if the rear face were maintained at some low temperature. The measured value of the first peak is about 25% lower than the calculated one. This ratio was also obtained for external radiant fluxes of 25, 75, and 100 kW/m^2. The second peaks are lower than the first peaks for the measured curves. This is partly due to the heat absorbed by the insulated backing board in the calorimeter. When the calculations were repeated using a heat of pyrolysis of 400 kJ/kg instead of zero the second peak was lower than the first peak and the first peak was closer to the measured value. The agreement is better than should be expected at this stage of the development of the model which needs better input data on the thermal properties at high temperature.

The calculated effective heat of combustion was approximately 12 MJ/kg which is the average value of the heat of combustion of the vapor over the full range of decomposition of the solid. It actually fell slowly with time and then rose rapidly as the final stage of char formation was approached. Except for the shift in time scale the agreement between calculated and measured values is within 25%.

DISCUSSION

For the limited comparisons made, the predicted and measured effective heats of combustion are very close. It is nearly constant at about 12 MJ/kg and independent of incident flux. The gross heat of combustion of the wood is 20 MJ/kg. The net heat of combustion after correcting for the evaporation of water is 18 MJ/kg. The much lower effective heat of combustion is due to dilution by the

TABLE 1. Input Data for Running the Model for Douglas Fir Particle Board

Property	Value	Source
Wood		
Activation Energy	121 kJ/mol	1
Pre-Exponential Factor	5.94×10^7 s^{-1}	1
Heat of Pyrolysis	0	2
Original Density	$709 kg/m^3$	1
Heat Capacity	$1.11 (1 + 0.0067 T-273) \times (0.54 + 0.46Z)$ kJ/kg.K	3
Thermal Conductivity	$1.24(0.35 + 0.65Z) \times (1 + 6.8(T-To) \times 10^{-4}) \times 10^{-4}$ kW/m.K	1
Absorptivity	0.8 $Z > 0.75$; 1.0 $Z < 0.75$	1
Contraction Factors*	$\ell_x = \ell_y = \ell_z = 1$ for $0.65 \leq Z \leq 1$ $= (0.65 - Z)^2$ for $Z < 0.65$	1a
Final Char Yield	0.22	1
Volatile Pyrolysis Products		
Heat Capacity	$1.05 + 1.80 \times 10^{-4}(T-273)$ kJ/kg.K	4
Heat of Combustion	20 [1.24 - Z] MJ/kg	1
Water		
Activation Energy	44 kJ/mole	4
Pre-Exponential Factor	4.5×10^3	4
Heat of Vaporization	2400 kJ/kg	4
Heat Capacity	4.19 kJ/kg.K, $T < 373$; $4.19 + 3.1 \times 10^{-5}(T-373)^2$ kJ/kg.K, $T > 373$K	5

1 Experimentally determined in this project.

2 Assumed.

3 Temperature Dependence - Koch [6]; dependence on charring assumed based on published value for charcoal.

4 Atreya [3].

5 Based on data in reference 7.

* The contraction factors were found to be independent of direction along the surface. They were assumed to be the same through the depth. Departure from unity for contraction factors with $Z > 0.65$ were within the scatter of the data.

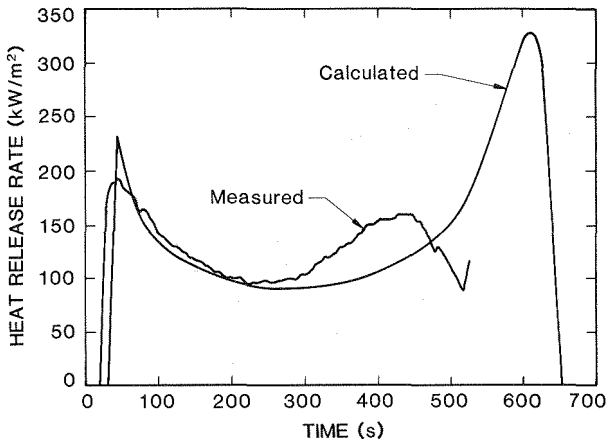

FIGURE 2. Heat release rate of dry Douglas fir particle board at an external radiant flux of 50 kW/m^2.

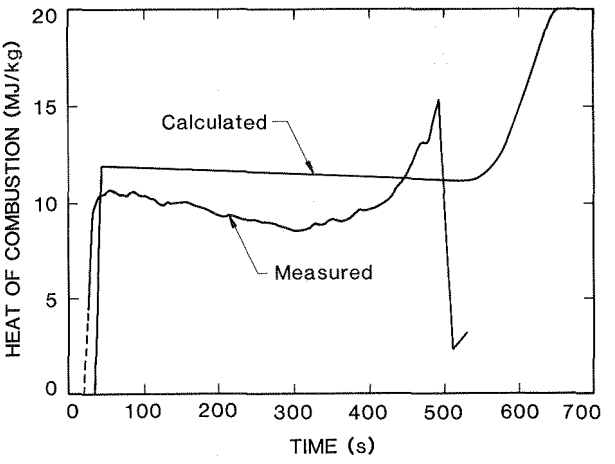

FIGURE 3. Effective heat of combustion of dry Douglas fir particle board at an external radiant flux of 50 kW/m^2.

water released in the char forming process. The initial peak heat release rates are within 25%. The shape of the calculated and measured heat release rate curves are similar but the time scales are substantially different. This may be due to inadequate data on the thermal properties of the char at high temperature, the assumption of a single first order reaction for wood or any of the several assumptions used in the construction of the model.

This computer model is unique in that it (1) accounts for the change in the heat of combustion of the volatiles generated during the pyrolysis period, (2) accounts for char shrinkage, and (3) provides for different reaction rates for the different components of wood. However this last capability was not exercised during this first test of the model where a single first order reaction was assumed. This is the standard assumption used in the mass loss rate models.

As this work continues, improvements will be made in the model and in the experimental methods employed to obtain the input data. Furthermore a much broader data base will be obtained on the thermophysical and thermochemical properties of wood and wood char particularly at high temperature. In order to reliably describe the kinetic constants for the thermal decomposition of wood and the effective heat of combustion of its volatile pyrolysis products as it evolves with time it will be necessary to make these determinations on the individual wood components (cellulose, hemicellulose, and lignin).

ACKNOWLEDGMENT

This work was suported in part by the Federal Emergency Management Agency.

REFERENCES

1. Kung. H.C., "A Mathematical Model of Wood Pyrolysis," Combustion and Flame, Vol. 18, pp 185-195(1972).

2. Tamanini, F., "A Study of the Extinguishment of Wood Fires," Ph.D. Thesis, Harvard University, May 1974.

3. Atreya, A., "Pyrolysis, Ignition, and Fire Spread on Horizontal Surfaces of Wood, Ph.D. Thesis, Harvard University, May 1983.

4. Barauskas, V., "Development of the Cone Calorimeter - A Bench-Scale Heat Release Rate Aparatus Based on Oxygen Consumption," NBSIR 82-2611, Nat. Bur. Stand. (U.S.), Nov. 1982.

5. Parker, W. J., "Development of a Model for the Heat Release Rate of Wood A Status Report," NBSIR (to be published), Nat. Bur. Stand. (U.S.) 1985.

6. Koch, P., "Specific Heat of Oven-Dry Spruce Pine Wood and Bark," Wood Sci. 1:203-214, 1969.

7. Weast, R.C., Editor, "Handbook of Chemistry and Physics", 57th edition, 1976-1977, pp. D158-D159.

NOMENCLATURE

A	frequency factor (s^{-1})
B	mass transfer number
C	heat capacity (kJ/kg.K)

E	activation energy (kJ/mole)
F	heat combustion of volatiles (kJ/kg) (positive)
h	convective heat transfer coefficient ($kW/m^2.K$)
h_p	heat of pyrolysis (kJ/kg) (positive when heat is absorbed)
K	thermal conductivity (kW/m.s)
ℓ	contraction factor
L_v	latent heat of vaporization of water (kJ/kg) (positive)
m	mass (kg)
n	number of components
N	number of subdivisions of the specimen
$\dot{q}''_e$	external radiant flux (kW/m^2)
$\dot{q}''_{fR}$	flame radiation to the surface (kW/m^2)
$\dot{q}''_{rel}$	rate of heat release (kW/m^2)
R	gas constant (8.314 kJ/mol/K)
t	time(s)
T	temperature (K)
Z	mass retention fraction
α	absorptivity and emissivity
Δt	time step (s)
Δx	thickness of each slice (m)
ω	defined by equation (14)
ρ	density (kg/m^3)
σ	Stefan Boltzmann constant 5.67×10^{-11} ($kW/m^2.K^4$)